Supplemental Materials

Tunable defect patterns induced by a low-frequency electric field in ferroelectric nematic liquid crystals

Natalia Podoliak, Lubor Lejček, Martin Cigl, and Vladimíra Novotná*

Institute of Physics of the Czech Academy of Sciences, Na Slovance 1999/2, 182 00 Prague 8, Czech Republic

S1. Experimental observations

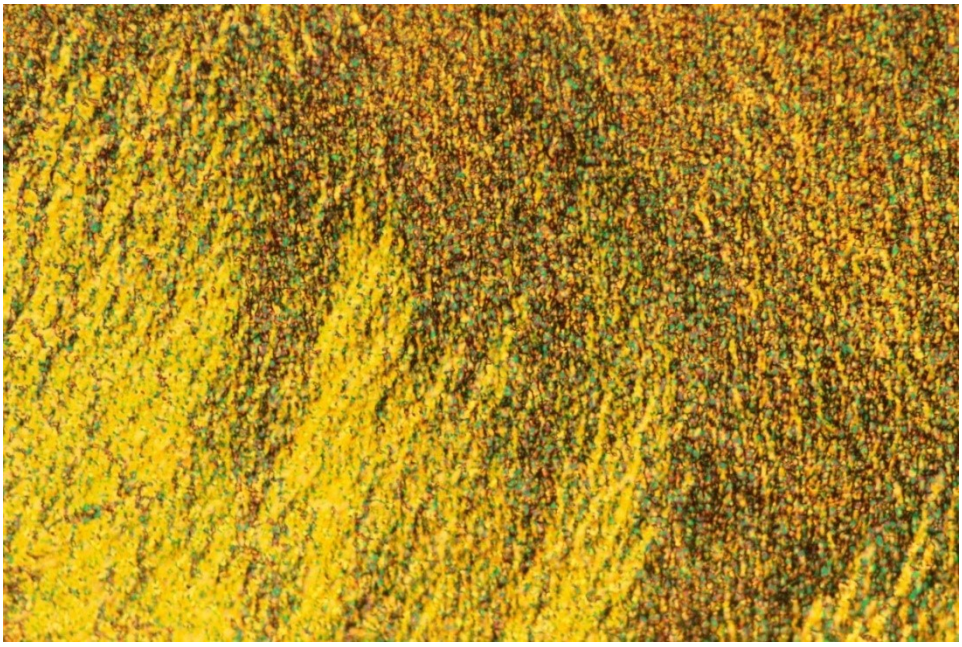

Figure S1. POM image of the virgin texture of a 5-μm HT sample in N_F phase, obtained after cooling from the Iso phase. The width of the photo is 950 μm, crossed polariser and analyser are along the edges of the photo.

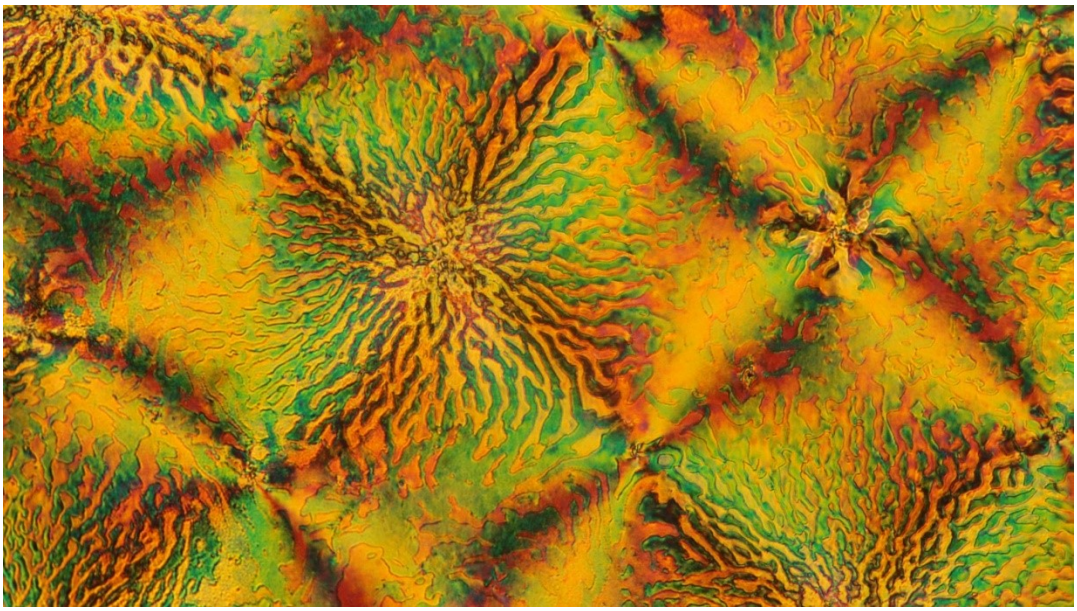

Figure S2. POM image of the studied sample after switching off the field. The appearance of smaller domains within the initial pattern is observed. Crossed polariser and analyser are along the edges of the photo. The width of the photo is 250 μm.

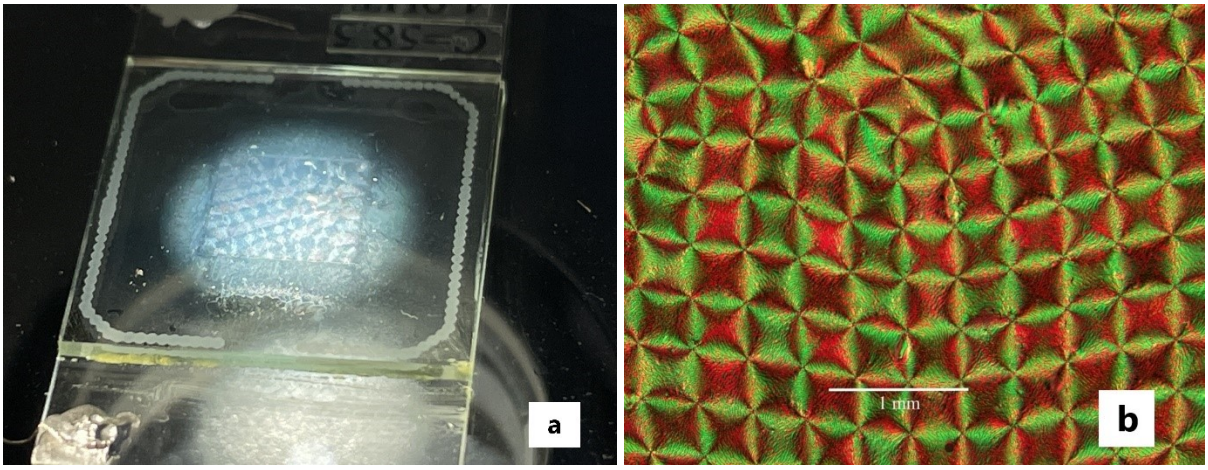

Figure S3. 5-μm HT sample in N_F phase after the application of 1 Hz AC electric field. a The photo of the studied sample. Large periodic domains are observed in the electrode area by naked eye. **b** POM image of the obtained pattern texture. Crossed polariser and analyser are along the edges of the photo. Scale bar corresponds to 1mm.

As a part of Supplemental information, videos presenting the pattern modification with the change of the applied field frequency are available. Video 1 shows the pattern reconfiguration while the frequence changes from 100 Hz to 10 Hz; Video 2 shows the pattern change for the frequency changing from 10 Hz to 1 Hz; Video 3 shows the pattern evolution for the subsequent change of frequency 1Hz – 10 Hz – 100 Hz. All the videos are taken at RT. One can see that for higher frequencies the pattern reconfiguration is slower.

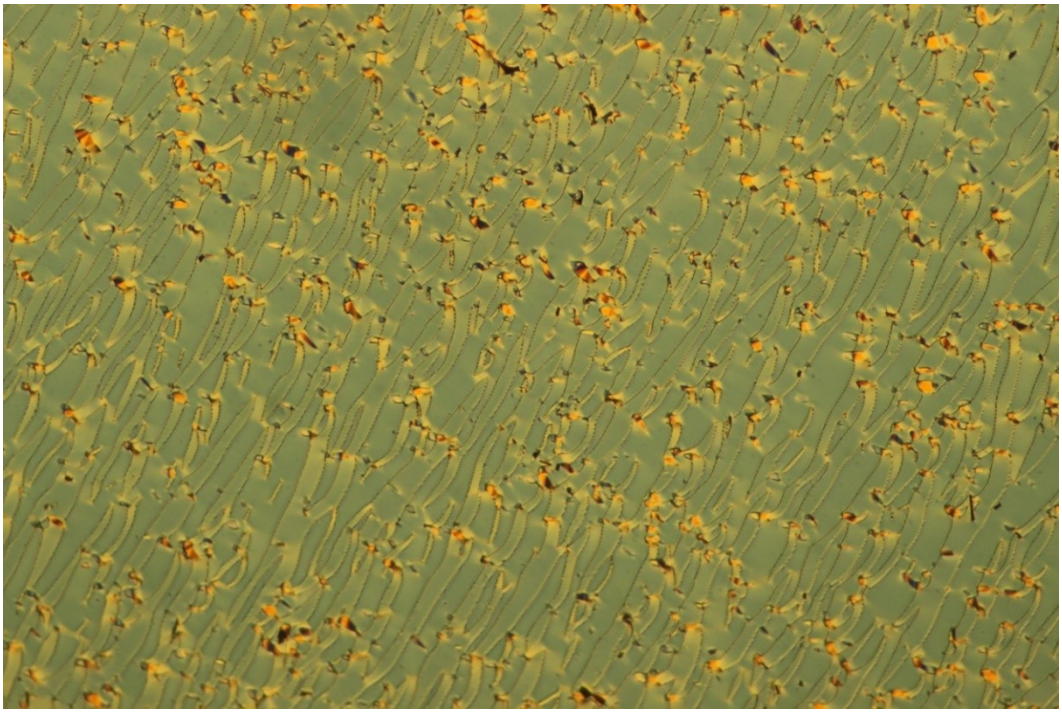

Figure S4. 5-µm HG sample with antiparallel molecular anchoring at the surfaces in the N_F phase. The texture is obtained after cooling from the Iso phase into N_F phase prior to the AC field application. It contains twisted domains with boderlines decorated with point-defects. The width of the photo is 950 µm. Crossed polariser and analyser are oriented along the edges of the photo.

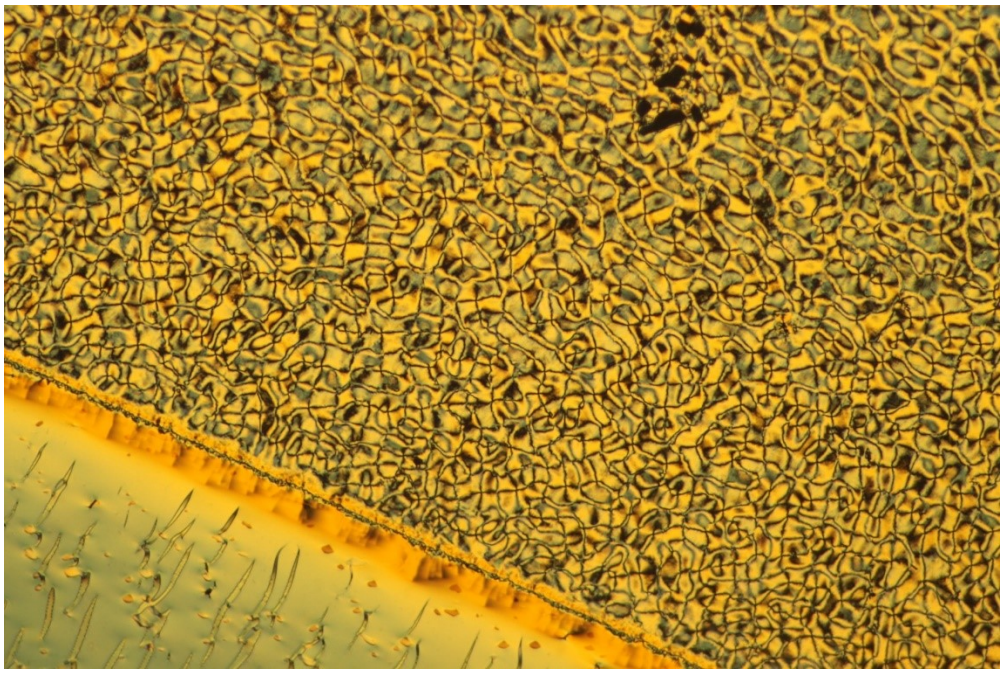

Figure S5. 1.5-µm HG sample with antiparallel molecular anchoring at the surfaces in the N_F phase after the application of 100 Hz AC electric field of the amplitude about 2.5 V/µm. The texture is obtained after cooling from the Iso phase into N_F phase and application of 100 Hz AC field of the amplitude about 2.5 V/µm. In the electrode area (upper right area of the microphotograph), a defect pattern is observed, while out of the electrodes (bottom left corner) former texture containing twisted domains perpendicular to the rubbing direction remained. The width of the photo is 950 µm. Crossed polariser and analyser are oriented along the edges of the photo.

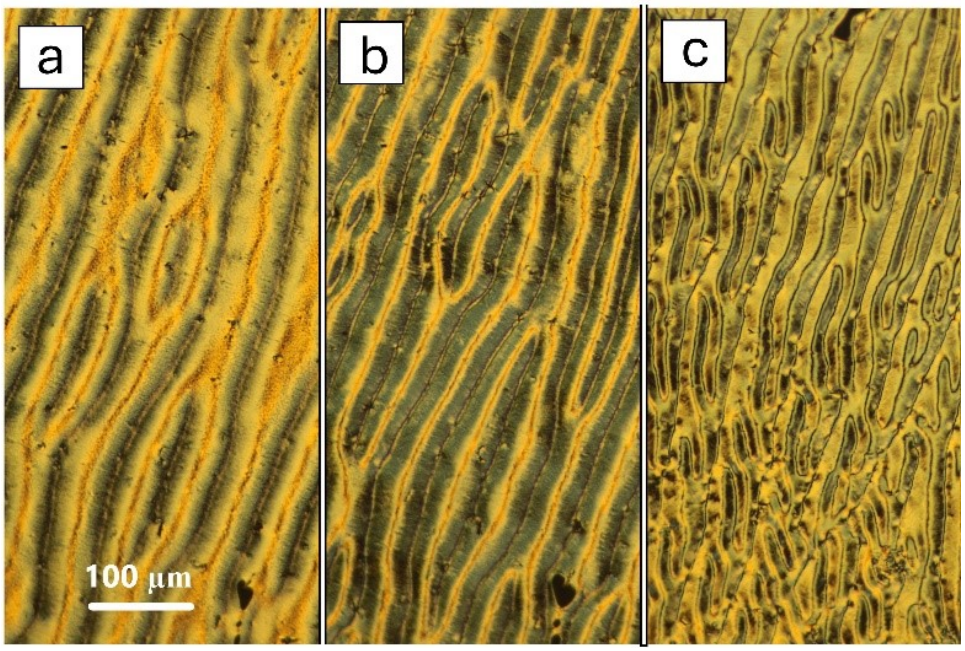

Figure S6. The stripe textures obtained in thin 1.5-µm HG cell with antiparallel rubbing at the surfaces, generated by small amplitude applied field of 1 V/µm of frequency: **a** 10 Hz; **b** 20 Hz; **c** 50 Hz. Crossed polariser and analyser are oriented along the edges of the photos. Scale bar corresponds to 100 µm.

S2. Defect vibration: a simple model

In this section, we propose a simplified model describing the vibration of the charged defects, appearing in ferroelectric nematics in response to the application of an AC electric field $\vec{E}_o cos(\omega t)$ with the frequency ω. Electric field interacts with the material spontaneous polarisation $\vec{P}_S$ as $\vec{P}_S \vec{E}_o cos(\omega t)$. Spontaneous polarisation $\vec{P}_S$ relates to the molecular director $\vec{n}$ as $\vec{P}_S = P_S \vec{n}$. The electric field is perpendicular to the sample surfaces while the director is inclined from the z-axis at an angle α.

Let us consider the situation observed in the cells with HT surface boundary conditions, in which the director profile near the surfaces is nearly parallel to z-axis. As it is seen from Figure 3b of the main article, the length of the defect is determined by the area in which the molecular inclination α changes from zero to π and is denoted as l_z along *z*-axis. This inclination is caused by the polarity of the molecules and different interactions of the molecular heads and tails with the surface. Due to this, the splay appears in the cell bulk, bringing bound charges. With oscillating field, the charged defects are also oscillating between the surfaces. For simplicity, we suppose that the molecular inclination over the defect length l_z is constant and denote it as α_s. The angle α_s is the model parameter. As it is seen from the observation of the director distribution around the defect visualised in Figure 3, we can assume that the defects are 2π-disclinations resembling the one discussed in literature.[1]

The absolute value of the electric energy applied to the system, $\left|hP_S E_o cos(\alpha_S) cos(\omega t)\right|$, should be absorbed in the sample. The absorbed energy stimulates the creation of the disclination system and its stabilisation. We denoted the mean distance between the oppositely charged defects in defect lattice as q (see Figure 3 of the main article). On the area q^2 there is one uncharged defect and four quatres of the neighbouring charged defects, i.e. two defects in total (Figure 3a). Therefore, the defect density is $\frac{2}{q^2}$.

The absorbed energy is responsible for the creation of the defects limited by the outer radius *R* in the (x,y) plane and elongated along *z*-axis with the length l_z. The elastic self-energy of the defect is

$$E_{es} = l_z \pi K ln\frac{R}{r_c}, \qquad \text{(S1)}$$

where K is the elastic constant in one-constant approximation with r_c being the core radius.[2,3] We expect $R \ll q/2$ as from the experimental microscopic observations q was found to be of the order of hundreds of μm.

The disclination self-energy due to the disclination charge can be expressed as:[4]

$$\frac{1}{2\varepsilon_o \varepsilon_r}\iint \frac{\rho(\vec{r})\rho(\vec{r}')}{|\vec{r}-\vec{r}'|}dVdV' \approx \frac{Q^2}{2\varepsilon_o \varepsilon_r l_z^2}\int_{-\frac{l_z}{2}}^{\frac{l_z}{2}} dz \int_{-\frac{l_z}{2}}^{\frac{l_z}{2}} dz' \frac{1}{\sqrt{r_c^2 + (z-z')^2}} \qquad \text{(S2)}$$

with $l_z < h,$ and ε_o and ε_r the dielectric permittivity of vacuum and the relative permittivity, respectively. Configurational disclination charge Q can be determined as:[5]

$$Q \approx \pi(R - r_c) l_z P_S sin\alpha_s \qquad \text{(S3)}$$

The volume density of charges $\rho(\vec{r})$ is Q/V , with a certain volume containing the disclination, i.e. $V \sim \pi R^2 l_z$. For $l_z > r_c$ we can estimate the above double integral (S2) to be $\sim l_z \, ln\frac{l_z}{r_c}$. Then the charge disclination self-energy of the defect length l_z can be estimated as

$$E_Q = \frac{Q^2}{2\varepsilon_o \varepsilon_r l_z} ln\frac{l_z}{r_c}. \qquad \text{(S4)}$$

For simplicity, we neglect the defect interaction energies, which are either attractive or repulsive. Thus, we can suppose that they compensate each other in the disclination system. It

should be noted, however, that the interaction energies are important for the determination of the exact defect positions in the array. Thus, we take as the approximated total defect self-energy the expression:

$$E_S = l_z \pi K ln\frac{R}{r_c} + \frac{Q^2}{2l_z \varepsilon_o \varepsilon_r} ln\frac{l_z}{r_c}. \qquad \text{(S5)}$$

Under the influence of an alternating electric field acting on the molecular polarisation, the charged defects vibrate between the upper and lower glass surfaces. The defect vibrations are, in fact, the reorientations of the director in the volume V (see Video 4 for the visualisation of the molecular reorientation near the charged defects under the influence of the AC electric field). Let the vibrational velocity of the charged defects along *z*- axis be described by v. Velocity v is the mean velocity over the period $\tau = 2\pi/\omega$.

The defect vibrations are damped down by the liquid crystalline viscosity. We take the corresponding dissipation energy describing this damping in analogy with the dissipation energy derived for the wedge disclination.[3] The charged defects observed in the present research are $+2\pi-$ wedge disclinations of the length l_z moving with the constant velocity v along *z*- axis. The approach applied in the literature[3] can be adapted to our geometry. The dissipation energy of the defect is $\Phi = - F_S v$ with the friction force

$$F_S = - \pi l_z \gamma_1 ln\frac{R}{r_c} v \; . \qquad \text{(S6)}$$

The parameter γ_1 is the nematic rotational viscosity and the parameter R limits the region around the moving defect, where the change of the director orientation takes place. For this reason,

R is a dynamic parameter,[3] which can be compared with the diffusion length of the orientation changes $\frac{K}{\gamma_1 v}$. In our model, we expect R to be of the same order as R in the elastic self-energy.

As Φ is the dissipated energy per unit time, we will integrate Φ over the period $\tau = 2\pi/\omega$ to obtain the dissipation energy in the form $\int_0^\tau \Phi dt$. By integrating over the period of the field oscillations, we approach the stationary state.

As the charged defects vibrate under the influence of the AC electric field while the uncharged defects do not (see Video 5 for the schematic molecular reorientation near the uncharged defect under the applied field influence), and also because the charge energy contribution is large, we will neglect non-charged disclinations and take the defect density as $\frac{1}{q^2}$. In this case, the energy balance between the field energy on one side and the energy of the defect system on another can be written as:

$$\frac{1}{q^2}\left[\int_0^\tau \Phi dt + E_S\right] = \frac{1}{\tau}\int_0^\tau \left|hP_S E_o cos(\alpha_S) cos(\omega t)\right| dt \qquad \text{(S7)}$$

Equation (S7) describes the balance of the dissipation energy and the disclinations self-energy multiplied by their density $\frac{1}{q^2}$, and the mean value of the electric energy per unit surface of the sample over the period τ. The mean value of the right side of (S7) is:

$$\frac{1}{\tau}\int_0^\tau \left|hP_S E_o cos\alpha_s cos(\omega t)\right| dt = \frac{2}{\pi}\left|hP_S E_o cos\alpha_s\right| . \qquad \text{(S8)}$$

Nevertheless, in (S7) we neglected the interaction energies between the disclination system and the interaction energies of their electric charges. The elastic interaction energies and the charge interaction energies are small as the defect distances in (x,y)- plane are large and they are also mostly compensated because of the opposite signs.

To estimate the mean vibration velocity of the defect, it is necessary to evaluate the dissipation energy. We expect that the electric field interaction with the molecular polarisation around one defect, given by an expression

$$-(\pi R^2)\left(P_S E_o cos\alpha_s\right)cos(\omega t), \qquad \text{(S9)}$$

is mainly dissipated in the material. Let z be the position of the defect geometric centre on the z-axis and $\dot{z}$ is the momentary velocity of the charged defect vibrations and it is time dependent. We describe this dissipation by the temporary force $-\pi l_z \gamma_1 ln\frac{R}{r_c}\dot{z}$. Using this equation for the dissipation and (S9) for the electric interaction, we propose the equation:

$$-\pi l_z \gamma_1 ln\frac{R}{r_c}\dot{z} - (\pi R^2)\left(P_S E_o cos\alpha_s\right)cos(\omega t) = 0, \qquad \text{(S10)}$$

which means that the force of the electric field acting on the defect is dissipated by its movement.

As it is discussed in literature,[3] the velocity should be constant both in the dissipation force and in the dissipation energy to assure the stationary process. For this reason, we use (S10) to find the mean square of the velocity v^2 over the period τ, which is time independent:

$$v^2 = \frac{1}{\tau}\int_0^{\tau} (\dot{z})^2 dt = \frac{1}{\tau}\int_0^{\tau} \left(\frac{-(\pi R^2)(P_S E_o cos\alpha_s)cos(\omega t)}{\pi l_z \gamma_1 ln\frac{R}{r_c}} \right)^2 dt = \frac{1}{2}\frac{(\pi R^2)^2 (P_S E_o cos\alpha_s)^2}{\left(\pi l_z \gamma_1 ln\frac{R}{r_c}\right)^2} \quad \text{(S11)}$$

The mean value of the square of velocity in (S11) is thus a constant and it can be used in the dissipation energy.

The expression $\int_0^{\tau} \Phi dt$ in (S7) can be evaluated as:

$$\int_0^{\tau} \Phi dt = \pi l_z \gamma_1 ln\frac{R}{r_c} \int_0^{\tau} (\dot{z})^2 dt = \frac{\pi (\pi R^2)^2 (P_S E_o cos\alpha_s)^2}{\omega \left(\pi l_z \gamma_1 ln\frac{R}{r_c}\right)} \quad \text{. (S12)}$$

Note that the integration over the time interval $(0, \tau)$ in (S12) is simply multiplication by τ. In this simplified approximation, the oscillations of the defects between the upper and lower surfaces caused by the electric field are completely dissipated.

To use the equation (S10), we also should be sure that the defect vibrations can follow the field frequency.

The equation (S7) gives the mean distance between the defects in the form:

$$q = \sqrt{\frac{\pi}{2}} \sqrt{\frac{(\pi R^2)^2 (P_S E_o cos\alpha_s)}{\omega h l_z \gamma_1 ln\frac{R}{r_c}} + \frac{E_S}{h(P_S E_o cos\alpha_s)}} \quad \text{. (S13)}$$

Equation (S7) shows the dependence of $q \sim \sqrt{\frac{a}{\omega} + b}$ as the function of ω and is plotted in Figure 1f together with the experimental points. The parameters appearing in Equation (S13) are taken from the fitting to the experimental results and from the previous measurements.[6]

S3. Parameters of the model

This frequency characteristic means that the dissipation energy decreases with the field frequency increase as the defects cannot follow the field oscillations at higher frequencies. The theoretical dependence $q \sim \sqrt{\frac{a}{\omega} + b}$ shows that the defect density $\frac{1}{q^2}$ increases with ω, which is observed experimentally. For low frequencies, there is a slight discrepancy between the theoretical predictions and the observed experimental results. The value of q recalculated from Equation (S13) for $\omega = 1\ Hz$ $q \sim 540\ \mu m$ is higher than the experimentally observed one $q \sim 350$ μm. This might be as a result of all the simplifications we had accepted.

In this section, we list the model parameters used in the fit of (S13). For the elastic modulus we can take $K \sim 10^{-11} N$ from the literature.[3] The dielectric permittivity of vacuum is $\varepsilon_o =$ 8.854 $\times 10^{-12}$ F/m. For the liquid crystal NF6 used for the investigation,[6] we measured $\varepsilon_r \approx 10^4$ and the spontaneous polarisation $P_S \approx 4 \times 10^{-2}$ C/m^2. The value of electric field for which the defect texture is realised is $E_o \approx 10^7$ V/m.

The sample thickness is $h = 5 \times 10^{-6}$ m. Parameter l_z is the defect length along z-axis and we can assume approximately $l_z \sim 1.6 \times 10^{-6}$ m. Angle α_s is taken as a mean value of α in the

defect of the length l_z and we consider it to be $\alpha_s \sim \pi/4$. Other parameters, R and r_c we can take as $R \sim 10^{-6}$ m, and $r_c \sim 10^{-8}$ m. From the fit, the value of the rotational viscosity is $\gamma_1 \approx 0.5$ Pa. Thus, our fit gives the nematic rotational viscosity for about one order greater than the rotational viscosity of classical nematic compound[3] named MBBA. We can generalise this finding and expect that the viscosity of the ferroelectric nematics is higher than it is for classical nematogens.

S4. Discussion of the model

We based our model on the idea that the electric energy applied to the sample is absorbed in it resulting in creation of the regular system of charged and uncharged defects shown in Figure 3. The vibration of the charged defects is caused by the interaction of the alternating electric field and the spontaneous molecular polarisation. In the energy balance (S7), the defect self-energies and the corresponding dissipative energies are the terms principally absorbing the energy of an electric field.

We can propose the director mapping around the created system of defect. In Figure S7,

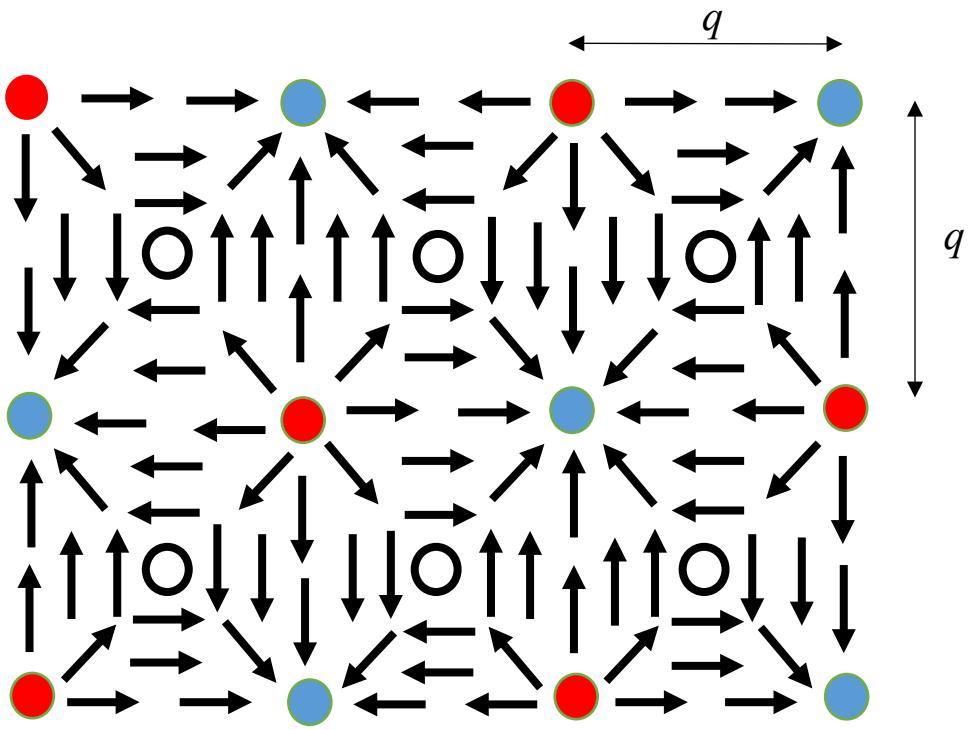

the schematic director organisation corresponding to the system of (±2π)-wedge disclinations is shown. $(+2\pi)$- disclinations are represented by the defects of different charge (red or blue points). Therefore, we see rows of $(+2\pi)$- disclinations with alternating charge signs with neighboring rows of (-2π)- disclinations without charge. Similar system of $(\pm 2\pi)$-wedge disclinations was observed across nematic-smectic phase transition.[1]

Figure S7. Schematic director organisation of the observed defect structure. Director organisation of the system of $(\pm 2\pi)$-wedge disclinations in the mid-plane of the sample. Arrows denote the orientation of the director and connected to it molecular polarisation. Coloured points are $(+2\pi)$- disclinations while white points are (-2π)- disclinations. Evidently, (-2π)-

disclinations are uncharged while $(+2\pi)$- disclinations have either positive or negative charges. Parameter q is the mean distance between the neighbouring defects.

In principle, we can propose another director field structure under the application of the electric field differing from the one shown in Figure S7. Note that the rotation of each director arrow at an angle π/2 gives a director map of $(\pm 2\pi)$-wedge disclinations without any charge (Figure S8). The self-energy (S5) of the charged defects is composed of their elastic self-energy and the energy of their charges. As the self-energy of the non-charged defects is just their elastic self-energy, it is evident that the creation of the charged defects absorbs more energy with respect to the non-charged defects. In our model, we neglected the interaction energies between the defects because the distances between them are of the order of hundreds of micrometres. Moreover, having alternating signs, they might probably mutually cancel. The energy of the electric field in the sample is absorbed by the defects self-energies and the vibration energies of the defects oscillating along the sample thickness, i.e. along z-axis. Due to this reason, we suggest that the observed defect structure corresponds to the one presented in Figure S7, and the structure of Figure S8 does not realise.

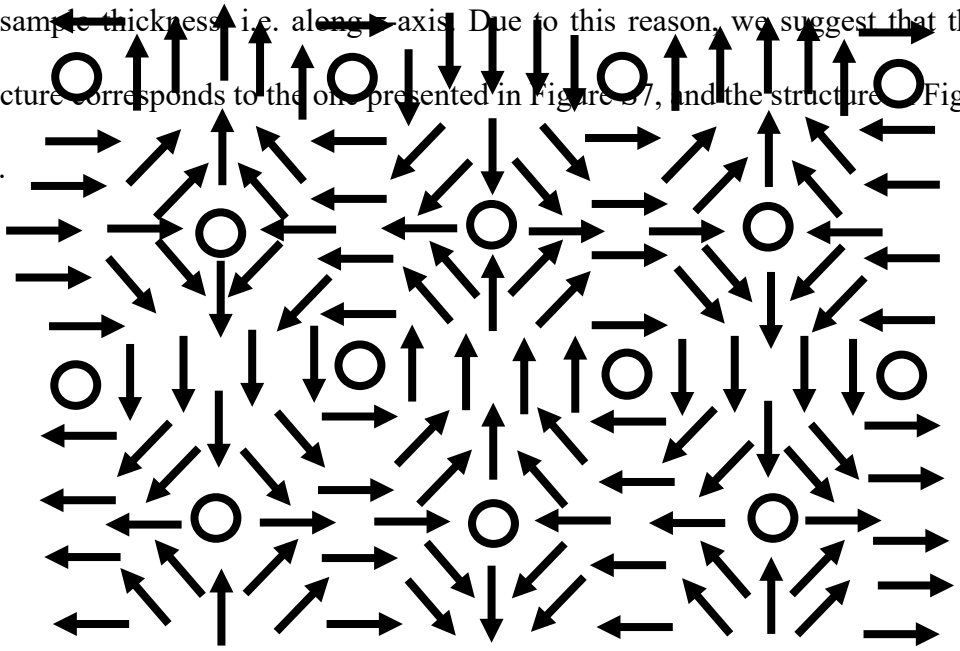

Figure S8. Alternative schematic director organisation of the observed defect structure. Director organisation of the system of $(\pm 2\pi)$-wedge disclinations in the mid-plane of the sample. Arrows denote the orientation of the director and connected to it molecular polarisation. It is seen from the director distribution that the disclinations are not charged. We consider this organisation energetically not favourable.

References:

[1] Wu, S.-B., Wu, J.-B., Cao, H.-M., Lu, Y.-Q. & Hu, W. Topological defect guided order evolution across the nematic-smectic phase transition. *Phys. Rev. Lett.* **130,** 078101 (2023).

[2] De Gennes, P. G. & Prost, J. *The Physics of Liquid Crystals* (Clarendon Press, Oxford, 1995).

[3] Oswald, P. & Pieranski, P. *Nematic and Cholesteric Liquid Crystals* (Taylor and Francis, Boca Raton, 2005).

[4] Jackson, J. D. *Classical Electrodynamics* (J. Wiley and Sons, New York, 1963).

[5] Lejcek, L. Twist disclinations in ferroelectric liquid crystals as sources of induced polarization space charges. *Ferroelectrics* **278,** 21-28 (2002).

[6] Cigl, M. et al. Giant permittivity in dimethylamino-terminated ferroelectric nematogens. *J. Mol. Liq.* **385,** 122360 (2023).